



Holocene sedimentary environment of a High-Arctic fjord in Nordaustlandet, Svalbard

Antti E.K. OJALA¹, Veli-Pekka SALONEN², Mateusz MOSKALIK³,
Frauke KUBISCHTA² and Markku OINONEN⁴

¹ *Geological Survey of Finland, Betonimiehenkuja 4, 02150 Espoo, Finland
<antti.ojala@gtk.fi>*

² *Department of Geosciences and Geography,
Gustaf Hällströmin katu 2a, 00014 University of Helsinki, Finland
<veli-pekka.salonen@helsinki.fi> <frauke.kubischta@myy.haaga-helia.fi>*

³ *Instytut Geofizyki, Polska Akademia Nauk,
ul. Księcia Janusza 64, 01-452 Warszawa, Poland <mmosk@igf.edu.pl>*

⁴ *Laboratory of Chronology, Finnish Museum of Natural History – LUOMUS,
Gustaf Hällströmin katu 2a, 00014 University of Helsinki, Finland
<markku.j.oinonen@helsinki.fi>*

Abstract: A 2.5-metre-long marine core from Isvika bay in Nordaustlandet (80°N, 18°E) was AMS ¹⁴C dated and analysed for its sedimentological and magnetic parameters. The studied record was found to cover the entire Holocene and indicates major turnovers in the palaeo-hydrography and sedimentary depositional history. The area was deglaciated at around 11,300 BP. The early Holocene has indications of rapid melting of glaciers and frequent deposition of ice-rafted debris (IRD). The climatic optimum terminated with a probable glacier re-advance event occurring *ca.* 5800 cal BP. This event caused the deposition of a diamicton unit in Isvika bay, followed by a shift towards a colder and a more stratified hydrographic setting. The reduction in IRD indicates gradual cooling, which led to the stratification of the bay and eventually to more persistent fast sea-ice conditions by 2500 cal BP. For the last 500 years, Isvika has again been seasonally open.

Key words: Arctic, Svalbard, Kinnvika, marine, sedimentology, climate change.

Introduction

The ongoing global climate change will have a severe effect on Arctic regions. The Arctic environment is rapidly changing. Annual and seasonal temperatures have been generally rising, and the sea-ice extent and volume have been declining with an ice loss unmatched in the last thousand years and unexplainable by any known natural variability (*e.g.* Solomon *et al.* 2007; Kwok *et al.* 2009; Polyak *et al.*

Pol. Polar Res. 35 (1): 73–98, 2014

2010). To understand such changes and relate them to changing natural environments, there is a need to investigate natural archives such as ice cores, lacustrine and marine sediments, especially at northern latitudes where the magnitude of expected change is the most pronounced and rapid (Holland and Bitz 2003; CAPE 2006; Miller *et al.* 2010). Such studies are valuable because they can provide proxy information on sea-ice coverage and its natural variations on a millennial timescale (*e.g.* Koç *et al.* 2002; Moran *et al.* 2006; Hald *et al.* 2007; Justwan and Koç 2008; Andrews 2009; Skirbekk *et al.* 2010; Werner *et al.* 2011).

Fjord sediments around the Svalbard archipelago record a complex relationship where temporally variable inputs from glaciers and their interactions with marine systems can be investigated (Cottier *et al.* 2010). The existing studies from Svalbard fjords have mainly been from the western, NW and southern coasts, and only a limited amount of information is available from the northern and eastern archipelago (Ingólfsson 2011). The physical environment of Kongsfjorden-Krossfjorden was investigated by Elvehøi *et al.* (1983) and Svendsen *et al.* (2002), who defined the factors driving the circulation and controlling sedimentation in the fjord system. Later, Zajączkowski *et al.* (2004), Zajączkowski and Włodarska-Kowalczyk (2007) and Zajączkowski (2008) compared sediment transport and settling in two fjords, glacial Kongsfjorden and outwash Adventfjorden, which are characterised by different transport systems. In the glacial-dominated Kongsfjorden, transport occurs as hypopycnal flows, with only limited sedimentation in the fjord environment, while in the non-glacial Adventfjorden, hyperpycnal transport and sedimentation leads to effective gravity flow and turbidite-type sedimentation of suspended material. In the Isfjorden area, Forwick and Vorren (2009) examined the sedimentary history, providing detailed information on varying sediment facies related to ice rafting and associated characteristic environments during the last 12,700 years. This approach was further developed in studies on Sassen- and Tempelfjorden in Spitsbergen (Forwick *et al.* 2010). Szczuciński *et al.* (2009) determined sediment accumulation rates in Billefjorden during the last 400 years. They demonstrated an up to ten-fold increase in the accumulation rate, which was interpreted to be the most pronounced sedimentary effect of ongoing climatic change.

Hornsund is the southernmost fjord in Spitsbergen, receiving meltwater from a number of tidewater glaciers. Majewski *et al.* (2009) investigated marine sediment cores from the mouth of Hornsund using high-resolution IRD, micropalaeontological and oxygen isotope analyses pointing out the significant role of Arctic and Atlantic water masses as pacemakers of the changing climate. In the north, Ślubowska *et al.* (2005) examined the postglacial history of Atlantic waters at the edge of the Arctic shelf at 80°N, and Batchelor *et al.* (2011) described how the active ice stream shaped the seafloor in Hinlopenstretet during the Late Weichselian. The fjords of Nordaustlandet had not been investigated in this respect at all before the studies of Kubischta *et al.* (2010, 2011).

As one of the activities of the International Polar Year 2007–2009, an expedition was organised to the Murchisonfjorden area, Nordaustlandet (Pohjola *et al.* 2011). Earlier studies by Kaakinen *et al.* (2009) and Kubischta *et al.* (2010) indicated that coastal sections in Isvika bay contain glacial and marine sediment sequences extending back to the beginning of the Weichselian glacial stage. The marine sediments of the bay could complement the geological history of the area, as was recently shown in the foraminiferal study by Kubischta *et al.* (2011). The present study aimed to produce background information on the presently prevailing water masses and their stratification and to explore the seabed conditions in Isvika bay in Murchisonfjorden. The second purpose was to provide a detailed marine sedimentological record from Isvika bay, and finally to discuss the sedimentary processes and changes in the sedimentary environment, palaeoceanographic settings and ice-rafting history of Murchisonfjorden since the Weichselian deglaciation.

Regional setting

Murchisonfjorden is an open bay about 15 km long and 10 km wide located at 80°N and 18°E (Fig. 1). It differs from a typical Svalbard fjord because it consists of a relatively shallow glacial archipelago without any longitudinal over-deepened glacially shaped depressions. The catchment is comprised of arctic desert with an annual precipitation about 400 mm of (Hagen *et al.* 1993), most of it as snow. The mean annual temperature is -8°C, and that of July about +3°C (Pohjola *et al.* 2011).

No tidewater glaciers presently terminate in Murchisonfjorden. However, the fjord receives glacial meltwaters from the Vestfonna ice cap and the main drainage is through the river Häggblomelva entering Sørvika bay (Fig. 1). Sea ice usually covers the fjord from October to June but there are marked year-to-year variations. Tidal currents were observed to raft icebergs to Murchisonfjorden through Hinloppstretet in the summer of 2007 and 2009.

The area was deglaciated during the Younger Dryas Stadial, 12,400–11,500 years ago (Kaakinen *et al.* 2009; Kubischta *et al.* 2011; Luoto *et al.* 2011). The landscape has a smoothly rolling topography, mostly covered by weathered rock debris. Glacial deposition has created a thin, discontinuous till blanket lacking any marked morphological features. Most of the remnants of glacial activity originate from the Mid-Weichselian Stadial, appearing as SE-NW oriented striations and linear bedrock forms. The Late Weichselian glacier in the area has been interpreted to have been dominantly cold-based, leaving only minor traces of its activity in the landscape (Kaakinen *et al.* 2009; Hormes *et al.* 2011).

Detailed bathymetric data reveal that the seafloor in Isvika bay has a flat central platform with steep slopes, especially on its northern side (Moskalik and Bialik 2011; Moskalik *et al.* 2012; see Fig. 2). The slopes show a linear topography caused by gullies and ridges. At the foot of the gullies there are a few semicircular forms

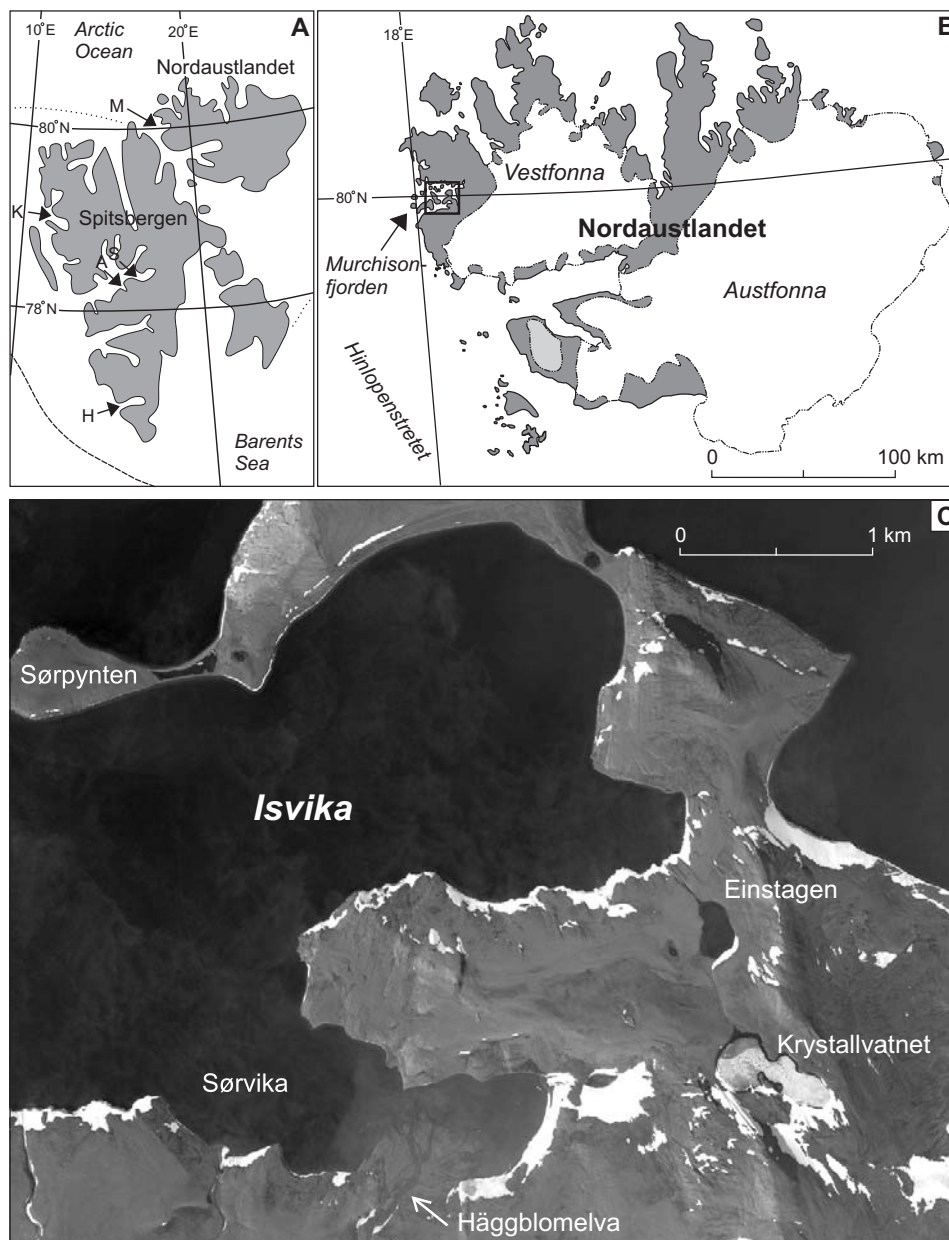


Fig. 1. The map of Svalbard (A) with the average limit of the Arctic sea ice marked with dashed (winter) and dotted (summer) lines (<http://nsidc.org/arcticseaicenews/>). The studied Isvika bay is located on the southeastern edge of Murchisonfjorden on Nordaustlandet, which is marked with a square (B). The aerial photograph (C) shows Isvika bay with a suspension plume entering the bay at the Hågblomelva river mouth. (The aerial photograph is courtesy of the Norwegian Polar Institute). (H – Hornsund, A – Adventfjorden, S – Sassen- and Tempelfjorden, K – Kongsfjorden-Krossfjorden, M – Murchisonfjorden).

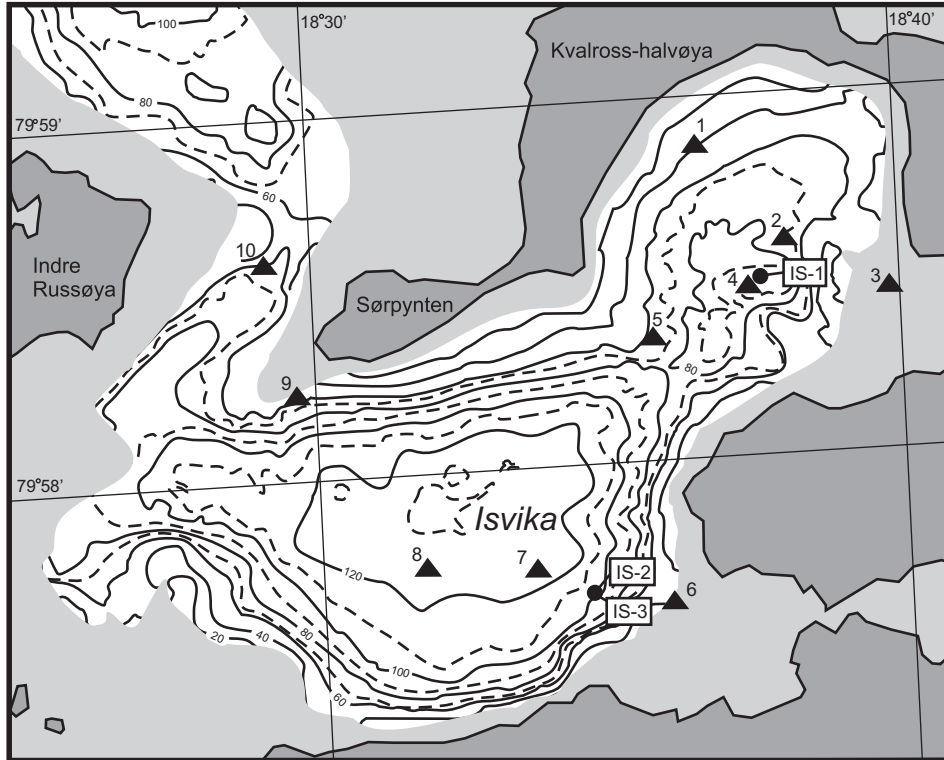


Fig. 2. Bathymetry of Isvika bay. Contour lines indicate water depths of 10 m (dashed) and 20 m (solid) (Moskalik *et al.* 2012), the coring locations (IS-1, IS-2 and IS-3) are marked with circles and CTD profile sites (1–10) with triangles.

probably associated with post-glacial debris events (Moskalik *et al.* 2012). The bottom topography is generally flat and lacking any distinct landforms or deposits, such as eskers, thrust moraines, glacial lineations and major mass-transport deposits, often described from other fjords in Svalbard (*e.g.* Howe *et al.* 2003; Ottesen and Dowdeswell 2009; Baeten *et al.* 2010; Forwick *et al.* 2010; Hogan *et al.* 2010). However, minor sediment creep structures are apparent on the SE slopes of Isvika bay, although they are limited in size and distribution (Moskalik *et al.* 2012).

Materials and methods

The marine sediment cores from the Isvika bay were collected onboard research vessel *Horyzont II* in August 2009. Before the retrieval of the cores, ten conductivity-temperature-depth (CTD) profiles were acquired using a Sea & Sun CTD 48M probe to obtain information on CTD variations of the water masses in Isvika bay (Figs 2, 3). Bathymetric data were collected using a motion-compen-

sated ELAC/SEA BEAM 1180 multibeam echosounder with hull-mounted transducers (Moskalik *et al.* 2012).

Altogether, three sediment cores were obtained using a modified Kullenberg piston corer with 350 to 500 kg weights and a core tube of 50 mm in diameter. Three coring attempts were performed at the eastern end of Isvika bay (IS-1, 79°58'30"N, 18°37'47"E, 95 m water depth), but a maximum of 34 cm of soft sediment were penetrated before the corer reached hard diamicton. The cores IS-2 (237 cm) and IS-3 (242 cm) were retrieved less than 50 m apart from each other from SW Isvika bay (79°57'43"N, 18°34'24"E) at a water depth of 100 metres. This second coring site was located within the area where a visible hypopycnal plume of turbidic water from the river Häggblomelva mouth enters the bay (Fig. 1).

The cores were sealed, stored at +4°C and transported to the sediment laboratory of the Geological Survey of Finland (GTK) in Espoo, where they were opened, halved and subsampled for further analyses. A visual description of the sediment characteristics was carried out immediately after opening. The water content was measured at 1-cm and loss on ignition (LOI) at 5-cm intervals from fresh sediment samples using standard methods (Bengtsson and Enell 1986).

Mineral magnetic parameters were used to support the sediment stratigraphical description and to detect changes that were not identified in the sediment visual characteristics (colour, structure, composition). Magnetic parameters were measured for a total of 68 subsample cubes (7 cm³) taken from cores IS-2 and IS-3. Low-field magnetic susceptibility (κ) was determined from the fresh sediment cores at 1-cm intervals using a Bartington MS2E1 surface-scanning sensor and from the subsample cubes using a Kappabridge KLY-2. Natural remanent magnetisation (NRM) and anhysteretic remanent magnetisation (ARM) were measured using a 2G-Enterprises SRM-755R tri-axial SQUID magnetometer. ARM was induced in each sample with a biasing direct field of 0.05 mT superimposed on a peak alternating field of 100 mT. Six samples from different lithological units (from depths of 20.5, 52, 74.5, 116, 180 and 242.5 cm) were selected for stepwise AF demagnetisation (0 to 120 mT peak AF) of NRM and ARM to determine the main carrier or the remanence. Following this, isothermal remanent magnetisation (IRM) acquisition curves were produced for the same six samples with a Molspin pulse magnetiser (from 25 to 1500 mT), and the remaining samples were exposed to a 1000 mT maximum field. IRM and SIRM were measured with a Molspin spinner magnetometer. Aside from dating, the mineral magnetic properties of sediments reflect the types, concentration and grain sizes of magnetic minerals in the sequence. Their down-core variations can be used for correlating sediment sequences and sometimes as a proxy for reconstructing past environmental changes (*e.g.* Thompson and Oldfield 1986; Oldfield 1991; Sandgren and Snowball 2001).

Mineral matter grain size variation was determined at 1-cm intervals. First, the sediment was wet sieved through mesh sizes of 1 mm, 0.1 mm and 0.063 mm

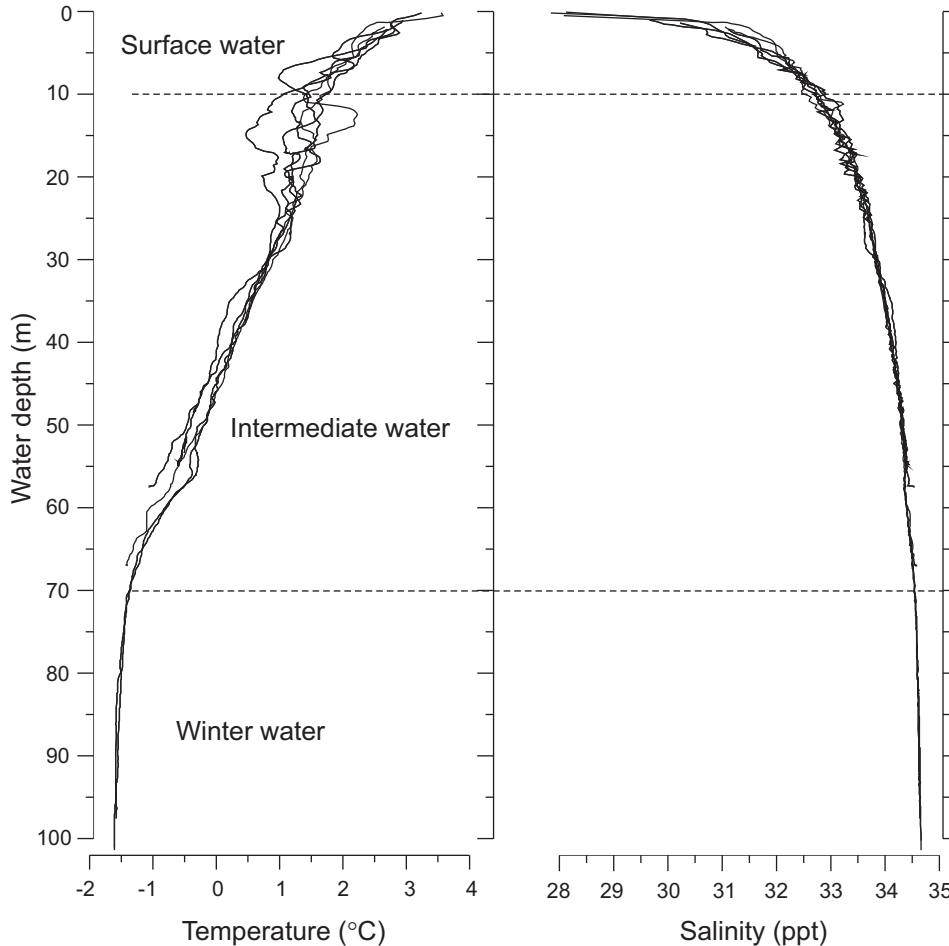


Fig. 3. Temperature and salinity variations for the Isvika area based on CTD profiles collected on 12 August 2009. Dashed horizontal lines indicate the vertical zonation of water masses into three layers.

in diameter, and the >0.1 mm fraction was then dry sieved to obtain the 0.5 mm fraction. All fractions were dried and their weight percentages measured. From the coarse fraction (>0.5 mm), all the grains were counted and classified under a stereomicroscope in order to sort the material into four components: lithic grains, plant remnants, shell fragments and foraminifer tests. The number of lithic grains (>500 μm) was used as an indicator of ice-rafted debris (IRD), which was reported as flux values ($\text{grains m}^{-2} \text{a}^{-1}$) using the bulk sediment density and rate of sedimentation.

The sediment age-depth model was based on 12 AMS ^{14}C measurements. Six samples represented single pieces of unidentified shell fragments and other six samples contained *ca.* 10 mg of a mixed sample of benthic foraminifera, excluding the epifaunal species *Cibicides lobatulus*, which is prone to re-deposition by

bottom currents (*e.g.* Knudsen *et al.* 2008). The age determinations were performed at the Laboratory of Chronology, Finnish Museum of Natural History – LUOMUS, University of Helsinki. The radiocarbon ages were corrected for isotopic fractionation and calibrated (cal BP) with the Oxcal program, version 4.1 (Bronk Ramsey 2009), which is based on the marine calibration data set (Marine 09; Reimer *et al.* 2009). In addition, a regional variation ΔR (Stuiver and Braziunas 1993) in the marine reservoir correction was estimated as a weighted average of the six tabulated ΔR values known within Svalbard (CHRONO Marine Reservoir Database <http://calib.qub.ac.uk/marine/>), and was found to be $\Delta R_{\text{Svalbard}} = 99 \pm 39$ (*e.g.* Mangerud *et al.* 2006).

Results and interpretation

Properties of the water masses

The water temperatures ranged from *ca.* +4°C at the surface to *ca.* -1.7°C in the deepest part of the basin (Fig. 3). The vertical salinity and temperature distribution revealed a stratified fjord with a distinct gradient within the uppermost 10 metres representing warm and less saline surface water. The temperature of surface water varied between +2 and +4°C and salinity from 29 to 33 ppt. The properties indicate the influence of terrestrial runoff from snowmelt, rivers and melting glaciers (Cottier *et al.* 2010). The vertical thickness of the thermocline varied from station to station between 8 and 15 metres (Fig. 3).

Below the surface layer was the intermediate water, where salinity increased and temperature decreased more slowly. Constant levels were reached at 70 metres depth, where another pycnocline separates the intermediate waters from winter-cooled waters (Fig. 3) (Nilsen *et al.* 2008). The winter-cooled water was stable, with the temperature ranging between -1.5 and -1.7°C and salinity being *ca.* 34.5 ppt.

Sediment stratigraphy

The sediment record from coring site IS-1 contained only 34 cm of mud, which was dark grey (N 3/0), folded and contained abundant granule and pebble size clasts. Beneath the mud, the corer hit a rocky diamicton, which could only be penetrated for a few centimetres.

Visual examination of sediment stratigraphy and *in situ* measurement of their magnetic susceptibility indicated that the core samples IS-2 and IS-3 contained the same sedimentary strata, which provided a solid basis for their correlation. As a consequence, a composite lithological log was created (Fig. 4) and the parallel cores were used for the analysis of physical properties and biological remains (Kubischta *et al.* 2011). In addition, about 15 cm of reddish clay material was re-

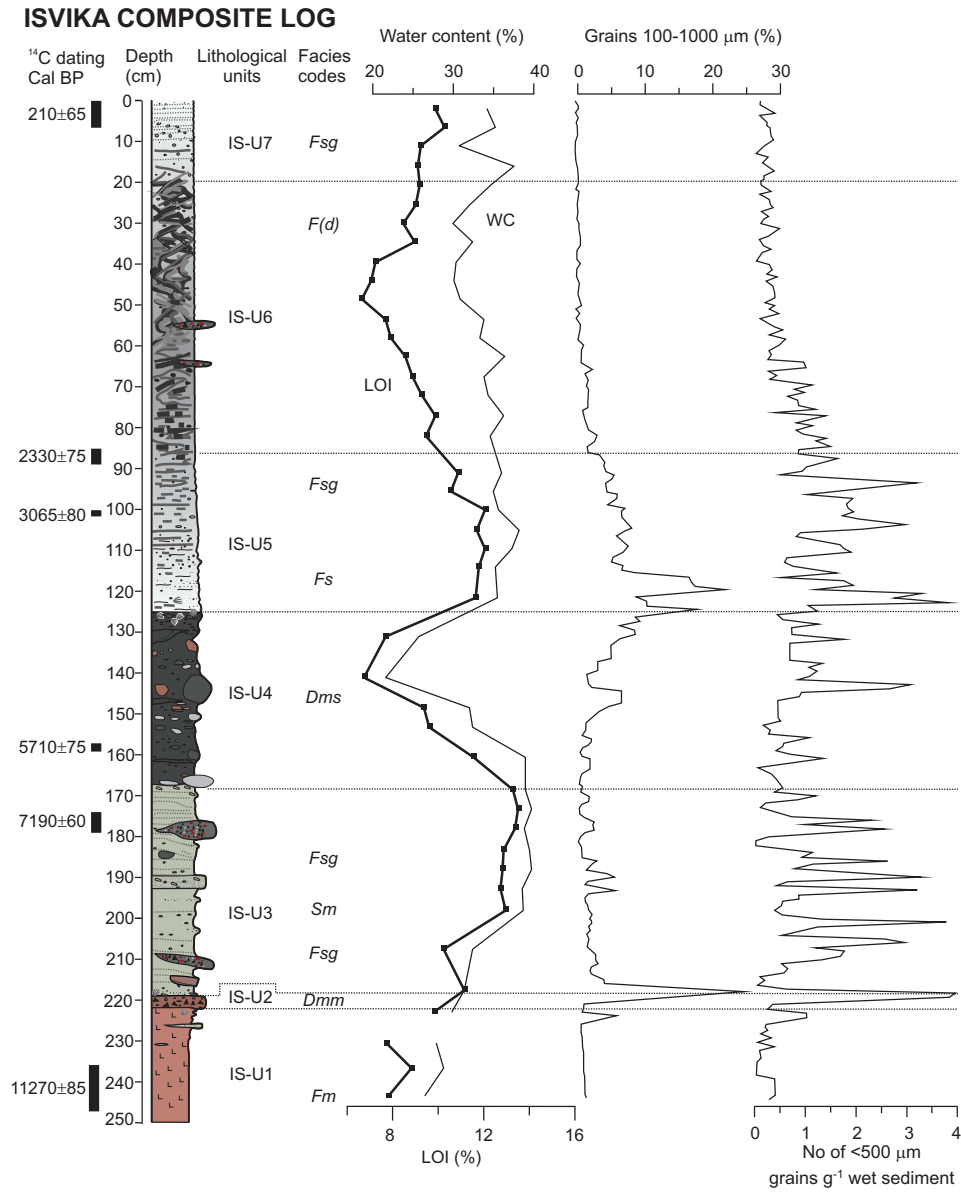


Fig. 4. A composite lithostratigraphical log based on the Isvika core sections IS-2 and IS-3 and their sedimentary LOI, water content and selected grain size profiles. The division into lithological units and facies codes within are given next to the log characteristics.

covered within the core catcher from the bottom of core IS-3, which was positioned as the lowermost part in the composite log and used in different analyses. When put together, the composite log was 250 cm long and the sequence was divided into seven different types of lithofacies based on their grain size, internal

structures, components, contacts and clasts occurrence (Smith and Andrews 2000; Eyles *et al.* 1983) (Fig. 4). These types are: (i) Fm – massive fine-grained mud, with occasional sand grains, (ii) Fsg – stratified mud with occasional granules and pebble size clasts, (iii) Fs – stratified mud with abundant sandy and granule layers, (iv) F(d) – deformed sulphide mud, with ebullition and gas escape structures, (v) Sm – massive fine grained sand, with small shell fragments, (vi) Dmm – matrix supported diamicton, and (vii) Dms – matrix supported diamicton, strongly stratified, with sand layers and shell fragments.

Age model and sedimentation rate

The sediment age-depth model is presented in Fig. 5 and is based on the mean values of selected and calibrated AMS ^{14}C probability curves. The oldest date obtained was 47,100 cal BP from a shell fragment at 52.5 cm sediment depth (Table 1). However, this can be considered as an outlier, because it is the only sample of Mid-Weichselian age lying in the middle of a likely Holocene section. The sample probably represents re-deposited material from an earlier interstadial sediment layer. The frequent occurrence of re-deposited shell material in the Murchisonfjorden area has earlier been noted in the Isvika catchment area by Blake (1961, 1989). In addition, typical Mid-Weichselian interstadial sands were AMS radiocarbon dated to *ca.* 40,000 cal BP in the Isvika stratigraphic sections by Kaakinen *et al.* (2009). Therefore, it is reasonable to assume that much of the shell material in the presently studied marine sediment sequence was re-deposited by glacial erosion and transportation during the deposition of diamicton units (*e.g.* unit IS-U4)

Table 1
Radiocarbon dates and calibrated ages of the foraminiferal tests and shell fragments determined from the Isvika bay core sections.

Lab ID	Core ID	Depth (cm)	Unit	Material	$\delta^{13}\text{C}$	^{14}C AMS age	Cal BP (68.2% range)	Cal BP (mean $\pm\sigma$)
Hela-2440	IS-2	3.5 \pm 3.5	IS-U7	Foraminifera	-0.7	687 \pm 25	150-280	210 \pm 65
Hela-2441	IS-2	39.5 \pm 0.5	IS-U6	Shells	-2.5	1113 \pm 25	550-635	590 \pm 40
Hela-2442	IS-2	52.5 \pm 0.5	IS-U6	Shells	-0.5	47101 \pm 971	47285 \pm 1015	
Hela-2443	IS-2	87 \pm 2	IS-U5	Foraminifera	-0.4	2739 \pm 29	2270-2410	2330 \pm 75
Hela-2607	IS-2	101 \pm 1	IS-U5	Foraminifera	-0.24	3342 \pm 33	2985-3155	3065 \pm 80
Hela-2444	IS-2	119.5 \pm 0.5	IS-U5	Shells	1.6	7634 \pm 33	7930-8045	8000 \pm 60
Hela-2445	IS-2	122.5 \pm 1.5	IS-U5	Shells	1.9	7471 \pm 36	7780-7910	7835 \pm 60
Hela-2606	IS-3	158.5 \pm 1.5	IS-U4	Foraminifera	-0.24	5506 \pm 47	5710-5865	5775 \pm 75
Hela-2446	IS-3	176 \pm 3	IS-U3	Foraminifera	-1.2	6758 \pm 32	7145-7250	7190 \pm 60
Hela-2447	IS-3	210	IS-U3	Shells	0.6	9085 \pm 36	9545-9725	9665 \pm 90
Hela-2512	IS-3	222.5	IS-U3	Shells	0.9	8952 \pm 38	9450-9550	9515 \pm 55
Hela-2511	IS-3	242.5 \pm 7.5	IS-U1	Foraminifera	-2.1	10374 \pm 42	11190-11310	11270 \pm 85

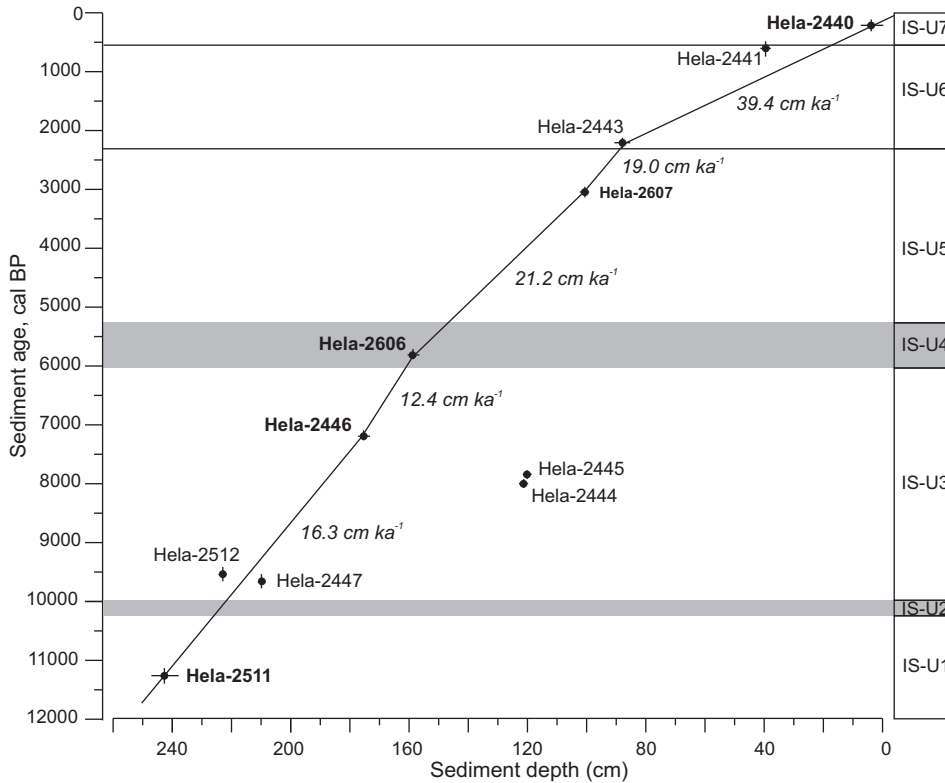


Fig. 5. Age-depth profile of the Isvika composite log used as an age model. Numbers indicate approximated rates of sedimentation per thousand years (cm ka^{-1}) based on calibrated AMS age determinations. Diamicton units are specified with gray.

and lenses. These ages thus have little value for establishing an age-depth model for the present sedimentary sequence. AMS ^{14}C ages derived from foraminiferal tests were found to be more reliable, and the present age-depth model is therefore solely based on these (Fig. 5 and Table 1).

The lowermost date from foraminiferal tests is from unit IS-U1 ($11,270 \pm 85$ cal BP) and can be considered as the bottom age of the presently studied Isvika sediment sequence. It also provides a minimum age for the deglaciation of the bay. It is somewhat younger than the age of deglaciation of the surrounding higher grounds, *i.e.* 12,400 cal BP (Luoto *et al.* 2011). Above this, the next two calibrated AMS ^{14}C ages lie at depths of 175–169 and 150–153 cm, and these are dated to 7190 ± 60 cal BP and 5775 ± 75 cal BP, respectively, providing a sedimentation rate of 12.4–16.3 cm ka^{-1} for the lower part of the sequence. The upper one of these two was collected from the diamicton unit (IS-U4) that was considered to have formed in a relatively short period of time. It was estimated that the duration of this event may have been only several hundreds of years, as the foraminiferal tests were collected from the whole unit IS-U4. They probably represent the taxa that were living on

the bottom of the bay, with an adjoining calving glacier margin depositing the melt-out till (Kubischta *et al.* 2011).

The uppermost three calibrated AMS ^{14}C dates that are based on foraminiferal tests are from depths of 100–102 cm (unit IS-U2), 85–89 cm (unit IS-U2), and 0–7 cm (unit IS-U1). They indicate respective ages of 3065 ± 80 cal BP, 2330 ± 75 cal BP and 210 ± 65 cal BP. Providing three linear trends based on these three dated horizons, we estimated that the rate of deposition was about 21.2 cm ka^{-1} between *ca.* 5800 and 3100 cal BP, about 19.0 cm ka^{-1} between 3100 cal BP and 2400 cal BP, and about 39.4 cm ka^{-1} after 2400 cal BP.

Lithological units

We identified seven lithological units that are each indicative of different environments in the history of Isvika bay. These units are described below.

Unit IS-U1 (250–222 cm). — This unit was dated at *ca.* 11,700 to 10,300 cal BP with a mean sedimentation rate of 16.3 cm ka^{-1} . It is composed of a grey-red (Munsell 2.5YR 4/2–5/2) massive mud with occasional sand grains. The lower contact was not reached. In the upper part, there are two greenish-red fine-grained sand patches, and a few 1-cm shells. Weak laminations are detectable, and granules and shell fragments lie on the top of the unit, where it changes with a gradual contact to unit IS-U2 above. Comparable “brick-red” clay with frequent sand grains was observed by Häggblom (1963) to represent the bottommost deglacial sediment in Krystallvatnet near the present study location (Fig. 1). Combined with sediment characteristics, the high dominance of *Cassidulina reniforme* and *Elphidium excavatum* and the low faunal diversity of foraminifera in IS-U1 (Kubischta *et al.* 2011) indicates that this unit was probably deposited by basal melting of the Late Weichselian glacier containing only very little debris material.

Unit IS-U2 (222–219 cm). — This unit was dated at *ca.* 10,300 to 10,000 cal BP and characterized by rapid sedimentation. It is a weak red (2.5YR 4/2) to dark grey (10YR 4/1) matrix-supported homogeneous diamicton. The clasts are very angular to angular and 1–3 mm in size, with a few 1-cm size pebbles at the base of the unit. The matrix is sandy and compacted, with a water content of about 20% (Fig. 4). Even though the unit is thin, it has many typical characteristics of till, such as poor sorting and clasts of angular shape with multiple lithologies. Moreover, most of the granules are reddish siltstones similar to rocks of the Celsiusberget Group (Sandelin *et al.* 2001) indicating a provenance from east and NE of Isvika bay. It can therefore be related to the uppermost Late Weichselian till unit described from the Isvika area by Kaakinen *et al.* (2009) which is known to indicate the final melting of the glacier ice in the Isvika area and associated melt-out deposition.

Unit IS-U3 (219–168 cm). — This unit was dated at *ca.* 10,000 to 6000 cal BP with a mean sedimentation rate of 12.4 to 16.3 cm ka^{-1} . It represents a heterogeneous series in which dark grey or greenish grey (5Y 4/1–2) and commonly faintly

stratified silty clay dominates and rests conformably on the unit below. In the bottom part (210–219 cm), there are large clasts and grey-coloured massive diamicton lenses, in addition to numerous granule-size clasts intermixed with the fine matrix. A few gas hollows can be observed at the sediment depth of *ca.* 200 cm, and a weak smell of sulphides was detected when opening the core. A 2-cm-thick sand layer with shell material lies at the level of 190–192 cm and a grey diamicton lens occurs at the depth of 178–180 cm. The top of the unit is distinctly stratified and sandy with a few shell fragments. LOI increases upwards from 10 to 13% and the water content of the sediment is about 40% (Fig. 4). The frequently occurring clast-dominated lenses and layers are probably indicative of the ice-rafting deposition, whereas the foraminifers indicate a more glacier-distal, but still high-arctic environment with increasing benthic productivity (Kubischta *et al.* 2011). In addition, appearance of *E. excavatum* and *Nonionellina labradorica* indicates an influence of normal-salinity open-ocean conditions (Kubischta *et al.* 2011).

Unit IS-U4 (168–125 cm). — This unit was dated at *ca.* 5500 to 6000 cal BP and characterized by rapid sedimentation. It has a loaded contact with unit IS-U3 below it. It was penetrated with both parallel cores and appeared with varying thicknesses. The unit is an olive grey (5Y 4/2), stratified, matrix-supported diamicton. The clasts are angular to subangular and represent various lithologies. The matrix is sandy and loose. There are thin sand lenses and layers throughout the series, especially in the top part of the unit. Shell fragments are abundant, and well-preserved shells dominate this coarse and sorted material at the top of the unit. The water content and LOI are the lowest recorded in the entire section (Fig. 4). Because the unit is matrix-supported and unsorted, the clasts being mainly angular and representing a wide variety of lithologies, the unit is interpreted as a melt-out till, which was deposited at or just beneath the glacier front. The clasts contain grey siltstones and dolomites of the Roalddalen Group (Sandelin *et al.* 2001), and the mineral magnetic properties of the unit point to an eastern-SE provenance for the material (Ojala *et al.* 2011). The basal contact is loaded without any significant signs of erosion. Moreover, the fine fraction contains intact foraminifer tests that have evidently been deposited *in situ*, thereby manifesting settling of this till unit from the glacier ice occupying Isvika bay. The faunal indication of foraminifera for the unit IS-U4 is not much different from that of the IS-U3, with the exception of high *Buccella frigida/tenerrima* appearance (Kubischta *et al.* 2011). That was interpreted as a result of redeposition whereas major part of the calcareous foraminifera represents an *in situ* assemblage living in this extreme environment (Kubischta *et al.* 2011).

Unit IS-U5 (125–86 cm). — This unit was dated at *ca.* 5300 to 2300 cal BP with a mean sedimentation rate of 19.0 to 21.2 cm ka⁻¹. It is very dark greenish grey (Gley1 3/1) sandy silt with abundant granule and shell material especially in the basal part. Towards the top, the material grades into a faintly laminated silty clay and becomes darker in colour. LOI values and the proportion of sandy mate-

rial are the highest in this unit (Fig. 4). Two ^{14}C dates from shell material (Hela-2444 and Hela-2445; Table 1) give ages older than the foraminiferal ^{14}C dates from the underlying unit IS-U4. This indicates that the lower part of unit IS-U5 probably contains re-deposited material, possibly related to slumping of the slopes or to the rain of ice-rafted debris. Unit IS-U5 was presumably deposited in ice-free open water under stable conditions. After the glacial ice melted, there was a continuous deposition of sand grains from ice rafts drifting into the bay. According to foraminiferal remains, the gradual increase of *E. excavatum* represents a transition to more severe condition and general cooling (Kubischta *et al.* 2011) towards the present day.

Unit IS-U6 (86–19 cm). — This unit was dated at *ca.* 2300 to 500 cal BP with a mean sedimentation rate of 39.4 cm ka⁻¹. It is dark grey to black (Gley1 2.5/N) mud with occasional sand granules. There are also two diamicton interclasts at the 65 and 55 cm levels. Gas hollows up to 1 cm in diameter are frequent in the lower part of the unit, at about 80 cm and 70 cm. The mud has sub-horizontal sulphide laminations at the base, but for the majority of the unit, the laminations are heavily contorted and folded to an extent that they have a “breccia-like” appearance. LOI values decrease simultaneously with the proportion of sand grains in the sediment. There is an apparent decreasing-increasing trend of LOI, probably reflecting variations in the relative proportion of inorganic material in the sediment. Sediment characteristics, combined with the decrease of *N. labradorica* (Kubischta *et al.* 2011), indicate a strong and possibly even permanent stratification of the water mass with more restricted or non-existent influence from open-ocean.

Unit IS-U7 (0–19 cm). — This unit was dated at *ca.* 500 cal BP to present with a mean sedimentation rate of 39.4 cm ka⁻¹. This uppermost unit represents the last centuries of sediment deposition and is characterised by olive grey (2,5Y 4/2) mud with occasional granules and clasts. The sediment is faintly laminated, with some sulphides present. The faunal diversity and increase of *C. lobatulus* in the upper part of this unit (Kubischta *et al.* 2011) might indicate a minor increase in the bottom current velocity in this site towards the present day.

Sediment magnetic properties

Sediment cores taken from Isvika bay were subsampled into 68 palaeomagnetic cubes (Fig. 6). Of these, only 20 cubes (from sediment depths 33–77 cm) provided a sufficient NRM intensity and stable inclination/declination signal for them to be used for palaeomagnetic dating. However, this section represents only around a thousand years of deposition, and it was thereby impossible to achieve meaningful information and resolution for sediment dating based on palaeosecular variations (*e.g.* Thompson and Oldfield 1986; Sandgren and Snowball 2001). Mineral magnetic parameters were consequently only used in sedimentological descriptions and interpretations.

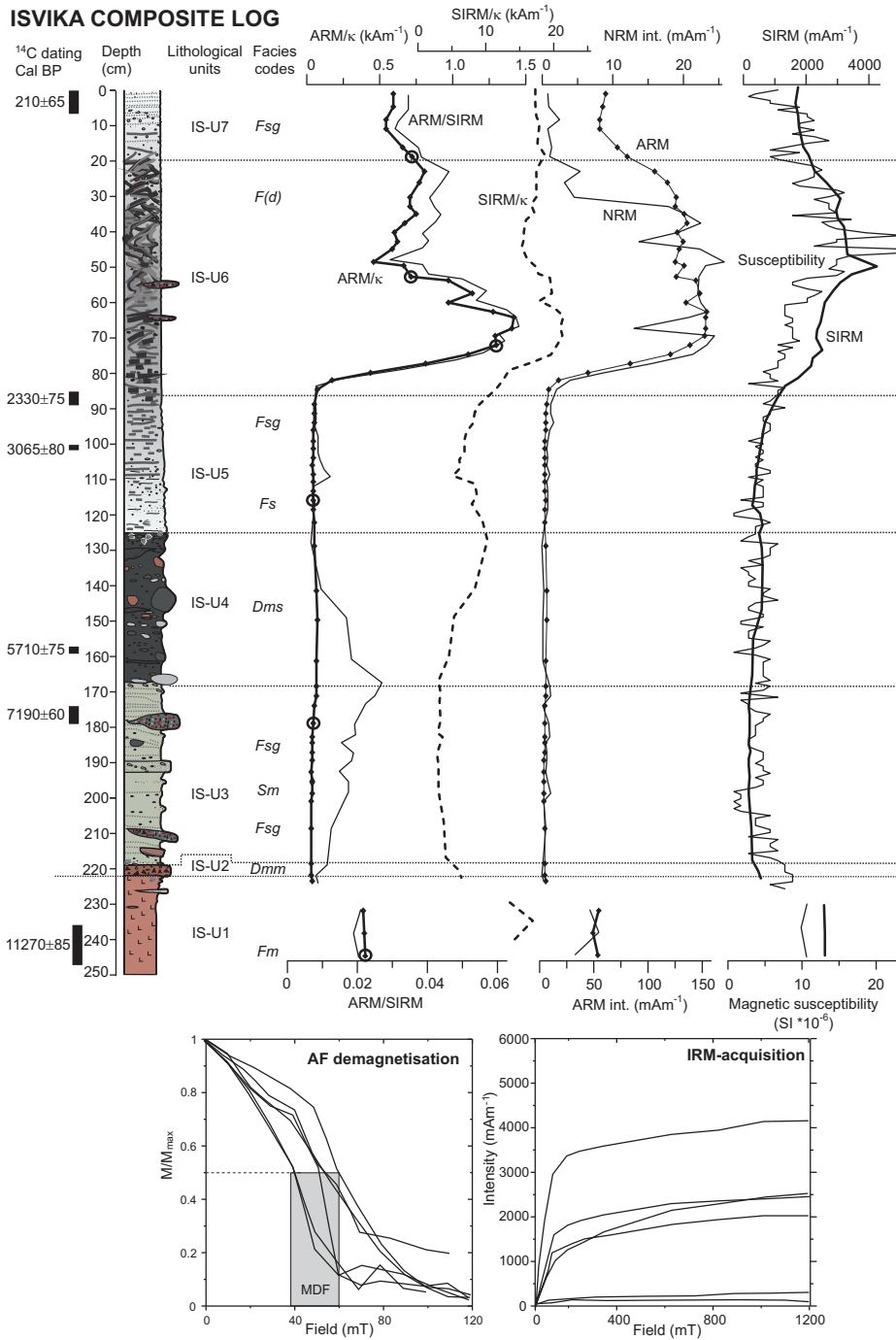


Fig. 6. The composite lithostratigraphical log plotted with magnetic mineral profiles measured at variable intervals. Black dots indicate magnetic sample cubes and those with circles around were measured for stepwise AF demagnetization and IRM acquisition.

Ojala *et al.* (2011) determined that the glacial sediments in the Murchisonfjorden area contain a fairly low concentration of the ferrimagnetic component and are dominated by higher coercivity canted antiferromagnetic mineral crystals, such as haematite and goethite. Based on AF demagnetisation and IRM acquisition curves, different depths of the Isvika bay section are dominated by a ferrimagnetic mineral, most likely magnetite, but they also contain a minor component of canted antiferromagnetic crystals. This is evidenced by the fact that the fraction of SIRM acquired above an IRM field of 200 mT is only about 5–15% and a median destructive field of NRM varies between 30 and 40 mT, depending on sample depth in the sequence (*e.g.* Thompson *et al.* 1980; Thompson and Oldfield 1986). Additionally, SIRM/k varies between 3 and 23 kAm⁻¹, which also suggests magnetite to be the dominant carrier of remanence in the section (*e.g.* Thompson *et al.* 1980). Down-core variation in the Isvika bay composite log indicates that mineral magnetic parameters remain relatively uniform at the depth of 90–220 cm with a very low magnetic mineral concentration. Three samples taken from the red clay in the lowermost part of the record (below 230 cm) have their own magnetic characteristics that are not found at any other depths in the sequence. In the upper 125 cm of the sediment core, magnetic susceptibility and SIRM are clearly negatively correlated with LOI. They indicate a maximum magnetic mineral concentration to occur between 30 and 60 cm.

The most substantial change in magnetic properties occurs at a depth of about 80 cm, where NRM and ARM intensities and mineral magnetic ratios (ARM/k and ARM/SIRM) show a sudden shift. They increase upwards to maximum values reached at the depth of about 65–70 cm. This characteristic feature is not seen this clearly in any other sediment physical parameter. As ARM is more sensitive to finer magnetite grains than susceptibility and SIRM, the increase in their ratios suggests a rapidly increasing dominance of finer magnetite grains. Above 65 cm, ARM/k and ARM/SIRM values decrease upwards more rapidly than the NRM and ARM intensities.

Discussion

Sediment sources. — The Isvika marine sediment record shows that the influence of major sediment sources, such as ice rafting, terrestrial input and biological productivity, has varied since the melting of the Late Weichselian continental ice sheet in the area. This is reflected in changes in the sedimentation pattern as well as the rate and composition of accumulated material in Isvika bay (Figs 4–6). Sediment structures and mineral magnetic parameters do not indicate any characteristics that could be related to sudden external physical processes such as slumping due to tectonics or considerable post-glacial erosion. The average rate of sedimentation for the whole post-glacial section in Isvika bay is about 22 cm ka⁻¹, which is

a typical Holocene value for Arctic fjords in the Svalbard region (*e.g.* Elverhøi *et al.* 1995; Forwick and Vorren 2009; Skirbekk *et al.* 2010). In the Isvika core, there are two major deviations from this the glacially influenced sedimentation event at about 5800 cal BP and the accelerated rate of sedimentation that was initiated at about 2500 cal BP.

The age-depth interpretation indicates that the bottommost sediment, the red clay unit IS-U1, was deposited at *ca.* 11,300 cal BP giving a minimum age for the initial deglaciation of the basin. The studied core section contains only a thin layer of reddish till (IS-U2), and it is the most probable that most of the deposits of the late Weichselian glaciation lying below IS-U1 in the basin were not recovered. The lowermost unit (IS-U1) contains abundant foraminiferal tests indicating a glacier-proximal setting as interpreted by Kubischta *et al.* (2011). This unit has a characteristic magnetic fingerprint representing a stable sedimentary environment that is distinctly different from any of the later deposits. Unit IS-U1 can be correlated with characteristic red clay found from the bottommost sediment in Lake Krystallvatnet, about 1 km SE of Isvika (Fig. 1). It was also interpreted to be of glacial origin by Häggblom (1963).

The fact that the composition of lithological unit IS-U2 resembles the uppermost Late Weichselian till unit described from the Isvika area by Kaakinen *et al.* (2009) suggests that this diamicton is associated with shore bank erosion and slump deposition from melting ice rafts. That could partly be due to shore-fast ice plucking and transporting material from the shore banks. Upon this lies unit IS-U3, which characterises the variable sedimentary environment of the early Holocene in the Isvika bay region. The frequently occurring coarser clasts and layers in unit IS-U3 are probably indicative of ice rafting deposition and at the same time the foraminifers indicate a more glacial distal environment with increasing benthic productivity (Kubischta *et al.* 2011). A gentle peak in the ARM/SIRM curve between *ca.* 10,000 and 6000 cal BP is contemporaneous with the increase in LOI and sediment water content, which, supported by the results from foraminiferal analyses (Kubischta *et al.* 2011), is interpreted as reflecting a period of warmer climate and higher productivity.

The diamicton at the core depth of 168–125 cm (unit IS-U4) was probably deposited by a glacier. The unit was found in both parallel cores with similar properties: a loaded base contact, characteristic sandy stripes and pods, a looseness of material and rounded to sub-angular clasts. The diamicton was dated to *ca.* 5800 cal BP from intact foraminiferal tests found *in situ* within the fine-grained matrix. The diamicton has all the characteristics of glaciomarine melt-out till that, on the basis of its mineral magnetic properties (Ojala *et al.* 2011), was deposited by a glacier advancing to Isvika from the east. The deposition of the unit IS-U4 might have been caused by a surge in Triodalen valley of the river Häggblomelva, but surging glaciers are unusual in the Nordaustlandet area (Hagen 1988) and no moraines in the valley or any other physical evidence on the sea floor support this interpreta-

tion (Moskalik *et al.* 2012). A slope failure (Forwick and Vorren 2007) would also explain the origin of the diamicton, but no chaotic sediment structures related to such debris were observed. The sediments display clear stratification and there is a continuous presence of foraminiferal accumulation and distinctive sediment load structures, which all indicate deposition from settling or dropping material. Our interpretation is that unit IS-U4 represents a glaciomarine deposit resulting from overall re-growth of the Vestfonna ice cap, which led to the proximity and possibly even a short-term overriding of a tidewater glacier in the Isvika area. Based on dating, this event occurred later than the well-known 8.2 ka climate cooling event (Alley and Augustdottir 2005), which has been found to have affected sedimentation as far north as Van Mijenfjorden, western Spitsbergen (Hald and Korsun, 2008). The Isvika re-advance event can be related to the overall mid-Holocene shift towards colder environments in the Svalbard region (*e.g.* Skirbekk *et al.* 2010). Similarly, Forwick *et al.* (2010) observed that the Tunabreen glacier in Tempelfjorden area rapidly advanced between 6000 and 4000 cal BP, and that there have been several events of glacier re-advance and retreat during the past two millennia.

The glacial sediments in the Isvika sequence are conformably overlain by glaciomarine muds (IS-U3, IS-U5, IS U-6 and IS-U7) containing a high but fluctuating amount of ice-rafted material (Fig. 7). The IRD flux is at its lowest in sediments (unit IS-U1) associated with deglaciation, which is unusual. Normally, the melting of glaciers produces the most ice rafting (*e.g.* Hald and Korsun 2008; Forwick and Vorren 2009) and highest number of grains. This indicates that in the Isvika area the melting glacier ice was very poor in debris, and probably for a long time after deglaciation there were no debris-rich ice rafts drifting into the bay. Another possibility would be that the low IRD content is related to cold fresh surface melt water that did not enable iceberg to melt close to the shore at that time. In any case, not until about 9500 cal BP did the sediments start receiving a regular, yet variable rain of IRD. This is indicated by occasional diamictic lenses in sandy mud, as well as an increased flux of IRD, averaging 400 grains $\text{m}^{-2}\text{a}^{-1}$.

The mid-Holocene glacial advance event caused a strong peak in the flux of sand grains, but sediments representing 5800 to 2500 cal BP again show a variable but stable IRD flux of about 400–500 grains $\text{m}^{-2}\text{a}^{-1}$. Since about 2500 cal BP there has been a decreasing trend in the IRD flux, with the last 500 years showing some variability. The decreasing trend can be seen from the proportional graphs of sand grains in sediment representing the core depths above 85 cm (Fig. 4). These sediment levels are also the most interesting features in the magnetostratigraphy. After 2500 cal BP, there is a clear increase in the appearance of finer-grained magnetite in the sediment section, which is often due to a change in the principal source of the sediment or an abrupt physical process perturbing the system or *in situ* chemical changes (Henshaw and Merrill 1980). Combined with other physical characteristics, these changes probably indicate that there was a contemporaneous increase in the rate of sedimentation mainly caused by finer-grained particles than those asso-

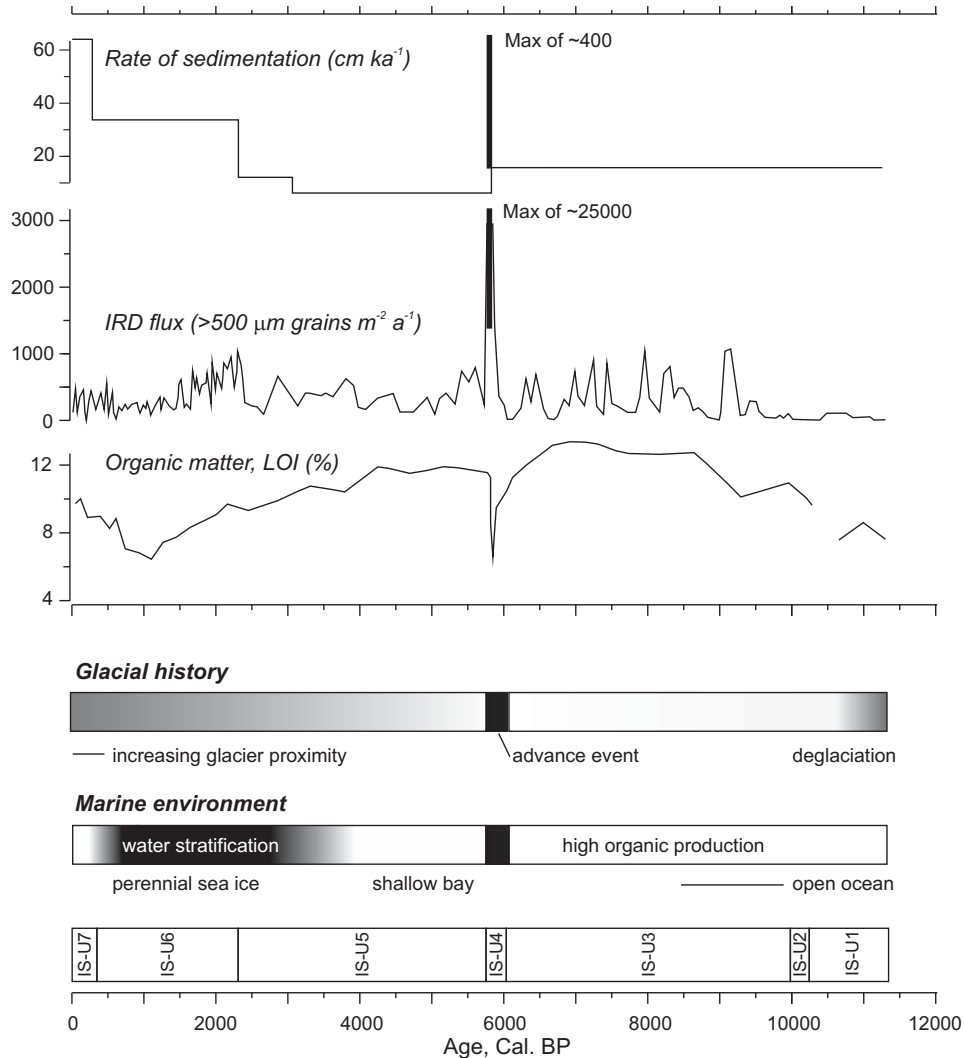


Fig. 7. Major trends in the sedimentation, glacial history and marine environment of the Isvika bay area during the Holocene. The large black arrows in the rate of sedimentation and IRD flux represent maximum peaks of these values, shading in glacial history and marine environment represent colder conditions and more stratified water masses, respectively.

ciated with IRD, *i.e.* suggesting increased sedimentation by suspension settling from a fluviially-derived component entering as overflow from Haggblomelva. Moreover, a reduced IRD flux could also result from suppressed ice-rafting deposition related to the enhanced formation of more shore-fast and/or permanent sea ice (Forwick *et al.* 2010). Finer-grained magnetite may also relate to the formation of authigenic magnetite or better preservation of finer magnetic grains in a sequence, both of which would suggest a clear change in the hydrography and chem-

ical deposition towards anoxic conditions. Several studies have shown that the formation of fine-grained magnetite in marine basins results from the appearance of magnetotactic bacteria, which live in the upper 10 cm of the sediments (*e.g.* Petermann and Bleil 1993; Pan *et al.* 2005; Lippert 2008). Magnetotactic bacteria generally live in the oxic-anoxic transition zone of aquatic environments, where dissolved oxygen and sulphide concentration are low and “bioavailable” iron is abundant (*e.g.* Lippert 2008).

The sediment was also observed to contain sulphides and a very high deposition rate of foraminiferal tests, especially in units IS-U5 and IS-U6 (Kubischta *et al.* 2011). Such an observation would imply higher productivity of the water body than on average during the Holocene. We found abundant hollows of up to 7 mm in size in the sediment at the level of *ca.* 200 cm and especially at the depth of 80–70 cm in the Isvika sediment sequences. These are probably gas-bubble structures, which can be connected to the activity of methanogenic bacteria indicating anaerobic conditions and slow decomposition of organic matter. The escape of trapped authigenic gas has then evidently caused the observed “sulphide breccia” sediment structures at depths of 20–80 cm. They resemble the soft sediment gas-escape structures that have been generated in laboratory experiments by Frey *et al.* (2009). The evidence of sediment methanogenesis, connected to the formation of fine-grained authigenic magnetite, again suggests that the Isvika bay had a strongly stratified water body and permanently stagnant water masses with anaerobic bottom conditions below the pycnocline, from about 2500 to *ca.* 500 cal BP (unit IS-U6). Near-bottom stratification appears in the fjords as a result of brine removal from the sea ice. Sinking brine fills basins and creates a pycnocline (Rasmussen and Thomasen 2009; Zajączkowski *et al.* 2010). In the Isvika area, this can be related to the more or less perennially frozen conditions, which continued until recent times. A similar situation has been described by Gallagher and Burton (1988) from Ellis fjord, Antarctica, where meromictic, hypersaline and anoxic conditions developed in closed basins of the fjord. Meromixis has therefore prevailed during the last 5000 years because the fjord is ice-covered for 11 to 12 months annually. The foraminifera record indicates a gradual mid- and late-Holocene cooling between *ca.* 5700 and 200 cal BP, but no direct indications were observed in the faunal diversity that could be related to stagnant bottom water and anaerobic conditions (Kubischta *et al.* 2011).

In the studied Isvika section, the topmost 1000 years again mark an increase in LOI, which may reflect the slower rate of bacterial mineralisation of the sediment organic matter and not necessarily an increase in organic deposition.

Palaeoenvironmental development of Murchisonfjorden. — Based on a record obtained from the northern Svalbard continental margin at the NW opening of Hinlopenstretet, the initial deglaciation took place *ca.* 15,000 cal BP (Koç *et al.* 2002; Ślubowska *et al.* 2005). The deglaciation initially proceeded slowly and the

catchment of Isvika bay was free of ice at around 12,400 cal BP (Luoto *et al.* 2011). Following this, the surface waters opened in Hinlopen Strait at *ca.* 11,500 cal BP or even as late as *ca.* 10,500 cal BP, according to Koç *et al.* (2002). In the Isvika area, this coincided with the final melting of glaciers and deposition of the reddish glaciomarine clay (unit IS-U1) at the beginning of the Holocene.

The post-glacial development of Isvika bay differs from that of other fjord records in Svalbard in many aspects, as summarised in Fig. 7. After the deglaciation the bay was in an open coastal setting, and organic production increased (Kubischta *et al.* 2011) during the early Holocene thermal optimum. The IRD record indicates the proximity of calving tidewater glaciers, and the sedimentation rate was very low, probably very similar to that observed in front of a cold-based glacier in Canada (Lemmen 1990). No evidence of a substantial cooling event around 8.2 ka could be detected in the present study, although it should be noted that this may also relate to insufficient resolution of the sediment cores IS-2 and IS-3.

The present results indicate a substantial glacier advance event with associated sediments during the mid-Holocene, and this marks a distinct turning point in the Isvika sedimentary record. Subsequently, the development towards cooler environments began, and the basin changed over to a closed bay with permanent stratification initiated about 2500 cal BP. In this sense, the sediment history also resembles that described from the high-Arctic Disraeli fjord (Lemmen 1990) on Herschel Island, or Ellis fjord, East Antarctica, where brine convection was responsible for producing hypersaline conditions at the bottoms of the two meromictic basins after the mid-Holocene (Gallagher and Burton 1988).

During the last 2500 years, the rate of sedimentation has been increasing, probably as a result of growth of the Vestfonna glacier and increased suspension settling of the fine sediments from the overflow. At the same time, the IRD flux has remained low, because the bay was probably covered by perennial sea ice for most of the time, thus preventing glacier rafts from drifting in. During the last 500 years, Isvika bay has again been seasonally open, and there are no further sedimentary indications of permanent anoxia.

Conclusions

Changing high-Arctic sedimentary environments were studied from two parallel sediment cores obtained within a fjord setting covering the entire Holocene Stage in Murchisonfjorden, Nordaustlandet. The record was dated with ^{14}C AMS and studied using sedimentological, magnetostratigraphical and IRD analyses. The sediment sequence reflects major turnovers in the palaeoceanographic development of the area:

- Deglaciation was dated close to the beginning of the Holocene, *i.e.* 11,300 cal years ago. Since then, the average rate of sedimentation (*ca.* 22 cm ka^{-1}) has remained rather low and stable.

- An open-ocean setting with increased organic production prevailed during the Early Holocene climate optimum.
- A glacier advance event culminated at about 5800 cal BP with the deposition of a glaciomarine melt-out till unit.
- After the mid-Holocene, gradual cooling finally led to permanent stratification of the basin, probably resulting from a more or less permanent perennial ice cover at about 2500 cal BP.
- Isvika bay has been seasonally ice-free during the last 500 years, with increased but highly fluctuating volumes of ice-rafted debris.

Acknowledgements. — We thank Captain Tadeusz Pastusiak and the crew of R/V *Horyzont II* for their support during the coring operation. The study was financed by the Academy of Finland (projects nos 1116709 and 259343) and was initiated as a part of the international IPY-Kinnvika project. The authors wish to acknowledge reviewers Marek Zajaczkowski and Jeremy Lloyd for helpful comments.

References

- ALLEY R.B. and AUGUSTDOTTIR A.M. 2005. The 8k event: cause and consequences of a major Holocene abrupt climate change. *Quaternary Science Reviews* 24: 1123–49.
- ANDREWS J.T. 2009. Seeking a Holocene drift ice proxy: non-clay mineral variations from the SW to N-central Iceland shelf: trends, regime shifts, and periodicities. *Journal of Quaternary Science* 24: 664–676.
- BAETEN N.J., FORWICK M., VOGT C., TORE O. and VORREN T.O. 2010. Late Weichselian and Holocene sedimentary environments and glacial activity in Billefjorden, Svalbard. *Geological Society, London, Special Publications* 344: 207–223.
- BATCHELOR C.L., DOWDESWELL J.A. and HOGAN K.A. 2011. Late Quaternary ice flow and sediment delivery through Hinlopen Trough, Northern Svalbard margin: Submarine landforms and depositional fan. *Marine Geology* 284: 13–27.
- BENGTSON L. and ENELL M. 1986. Chemical analysis. In: B.E. Berglund (ed.) *Handbook of Holocene Palaeoecology and Palaeohydrology*. John Wiley & Sons Ltd, Chichester: 423–451.
- BLAKE W. Jr. 1961. Radiocarbon dating of raised beaches in Nordaustlandet, Spitsbergen. In: G.O. Raasch (ed.) *The Geology of the Arctic*. University of Toronto Press, Toronto: 133–145.
- BLAKE W. Jr. 1989. Radiocarbon dating by accelerator mass spectrometry: A contribution to the chronology of Holocene events in Nordaustlandet, Svalbard. *Geografiska Annaler, Series A, Physical Geography* 71: 59–74.
- BRONK RAMSEY C. 2009. Bayesian analysis of radiocarbon dates. *Radiocarbon* 51: 337–360.
- CAPE – Last Interglacial Project Members 2006. Last Interglacial Arctic warmth confirms polar amplification of climate change. *Quaternary Science Reviews* 25: 1383–1400.
- COTTIER F.R., NILSEN F., SKOGSETH R., TVERBERG V., SKARDHAMAR J. and SVENDSEN H. 2010. Arctic fjords: a review of the oceanographic environment and dominant physical processes. *Geological Society, London, Special Publications* 344: 35–50.
- ELVERHØI A., LØNNE Ø. and SELAND R. 1983. Glaciomarine sedimentation in a modern fjord environment, Spitsbergen. *Polar Research* 1: 127–149.
- ELVERHØI A., SVENDSEN J.I., SOLHEIM A., ANDERSEN E.S., MILLIMAN J., MANGERUD J. and HOOKE R.LeB. 1995. Late Quaternary sediment yield from the High Arctic Svalbard area. *Journal of Geology* 103: 1–17.

- EYLES N., EYLES C.H. and MIALL A.D. 1983. Lithofacies types and vertical profile models; an alternative approach to the description and environmental interpretation of glacial diamict and diamictite sequences. *Sedimentology* 30: 393–410.
- FREY S.E., GINGRAS M.K. and DASTHGARD S.E. 2009. Experimental studies of gas-escape and water-escape structures; mechanisms and morphologies. *Journal of Sedimentary Research* 79: 808–816.
- FORWICK M. and VORREN T.O. 2007. Holocene mass-transport activity and climate in outer Isfjorden, Spitsbergen: marine and subsurface evidence. *The Holocene* 17: 707–716.
- FORWICK M. and VORREN T.O. 2009. Late Weichselian and Holocene sedimentary environments and ice rafting in Isfjorden, Spitsbergen. *Palaeogeography, Palaeoclimatology, Palaeoecology* 280: 258–274.
- FORWICK M., VORREN T.O., HALD M., KORSUN S., ROH Y., VOGT C. and YOO K.-C. 2010. Spatial and temporal influence of glaciers and rivers on the sedimentary environment in Sassenfjorden and Tempelfjorden, Spitsbergen. *Geological Society London, Special Publication* 344: 163–193.
- GALLAGHER J.B. and BURTON H.R. 1988. Seasonal mixing of Ellis Fjord, Vestfold Hills, East Antarctica. *Estuarine, Coastal and Shelf Science* 27: 363–380.
- HAGEN J.O. 1988. Glacier surge in Svalbard with examples from Usherbreen. *Norsk Geografisk Tidsskrift* 42: 203–213.
- HAGEN J.O., LIESTØL O., ROLAND E. and JØRGENSEN T. 1993. *Glacier Atlas of Svalbard and Jan Mayen*. Norsk Polarinstitutt, Oslo: 141 pp.
- HÄGGBLUM A. 1963. Sjöar på Spetsbergens Nordostland (Lakes in Nordaustlandet, Svalbard). *Bulletin of the Institute of Geography, University of Stockholm* 49: 76–105.
- HALD M. and KORSUN S. 2008. The 8200 cal. yr BP event reflected in the Arctic fjord, Van Mijenfjorden, Svalbard. *The Holocene* 18: 981–990.
- HALD M., ANDERSSON C., EBBESEN H., JANSEN E., KLITGAARD-KRISTENSEN D., RISEBROBAKKEN B., SALOMONSEN G.R., SARNTHEIN M., SEJRUP H.P. and TELFORD R.J. 2007. Variations in temperature and extent of Atlantic Water in the northern North Atlantic during the Holocene. *Quaternary Science Reviews* 26: 3423–3440.
- HENSHAW P.C. Jr and MERRIL R.T. 1980. Magnetic and chemical changes in marine sediments. *Reviews of Geophysics and Space Physics* 18: 483–504.
- HOGAN K.A., DOWDESWELL J.A., NOORMETS R., EVANS J. and COFAIGH C.Ó. 2010. Evidence for full-glacial flow and retreat of the Late Weichselian ice sheet from the waters around Kong Karls Land, eastern Svalbard. *Quaternary Science Reviews* 29: 3545–3562.
- HOLLAND M.M. and BITZ C.M. 2003. Polar amplification of climate change in coupled models. *Climate Dynamics* 21: 221–232.
- HORMES A., AKÇAR N. and KUBIK P.W. 2011. Cosmogenic radionuclide dating indicates ice-sheet configuration during MIS 2 on Nordaustlandet, Svalbard. *Boreas* 40: 636–649.
- HOWE J.A., MORETON S.G., MORRI C. and MORRIS P. 2003. Multibeam bathymetry and the depositional environments of Kongsfjorden and Krossfjorden, western Spitsbergen, Svalbard. *Polar Research* 22: 301–316.
- INGÓLFSSON Ó. 2011. Fingerprints of Quaternary glaciations on Svalbard. *Geological Society, London, Special Publications* 354: 15–31.
- JUSTWAN A. and KOÇ N. 2008. A diatom based transfer function for reconstructing sea ice concentrations in the North Atlantic. *Marine Micropaleontology* 66: 264–278.
- KAAKINEN A., SALONEN V.-P., KUBISCHTA F., ESKOLA K.O. and OINONEN M. 2009. Weichselian glacial stage in Murchinsonfjorden, Nordaustlandet, Svalbard. *Boreas* 38: 718–729.
- KNUDSEN K.L., SØNDERGAARD M.K.B., EIRÍKSSON J. and JIANG H. 2008. Holocene thermal maximum off North Iceland: Evidence from benthic and planktonic foraminifera in the 8600–5200 cal year BP time slice. *Marine Micropaleontology* 67: 120–142.

- KOÇ N., KLITGAARD-KRISTENSEN D., HASLE K., FORSBERG C.F. and SOLHEIM A. 2002. Late glacial paleoceanography of Hinlopen Strait, northern Svalbard. *Polar Research* 21: 307–314.
- KUBISCHTA F., KNUDSEN K.L., KAAKINEN A. and SALONEN V.-P. 2010. Late Quaternary foraminiferal record in Murchisonfjorden, Nordaustlandet, Svalbard. *Polar Research* 29: 283–297.
- KUBISCHTA F., KNUDSEN K.L., OJALA A.E.K. and SALONEN V.-P. 2011. Holocene benthic foraminiferal record from a high-arctic fjord, Nordaustlandet, Svalbard. *Geografiska Annaler, Series A, Physical Geography* 93: 227–242.
- KWOK R., CUNNINGHAM G.F., WENNAHAN M., RIGOR I., ZWALLY H.J. and YI D. 2009. Thinning and volume loss of the Arctic Ocean sea ice cover: 2003–2008. *Journal of Geophysical Research* 114: C07005.
- LEMMEN D.S. 1990. Glaciomarine sedimentation in Disraeli Fiord, high arctic Canada. *Marine Geology* 94: 9–22.
- LIPPERT P.C. 2008. Big discovery for biogenic magnetite. *Proceedings of the National Academy of Sciences* 105: 17595–17596.
- LUOTO T.P., NEVALAINEN L., KUBISCHTA F., KULTTI S., KNUDSEN K.L. and SALONEN V.-P. 2011. Late Quaternary ecological turnover in High Arctic Lake Einstaken, Nordaustlandet, Svalbard (80°N). *Geografiska Annaler, Series A, Physical Geography* 93: 337–354.
- MAJEWSKI W., SZCZUCIŃSKI W. and ZAJĄCZKOWSKI M. 2009. Interactions of Arctic and Atlantic water-masses and associated environmental changes during the last millenium, Hornsund (SW Svalbard). *Boreas* 38: 529–544.
- MANGERUD J., BONDEVİK S., GULLIKSEN S., HUFTHAMMER A.K. and HØISÆTER T. 2006. Marine ¹⁴C reservoir ages for the 19th century whales and molluscs from the North Atlantic. *Quaternary Science Reviews* 25: 3228–3245.
- MILLER G.H., ALLEY R.B., BRIGHAM-GRETTE J., FITZPATRICK J.J., POLYAK L., SERREZE M.C. and WHITE J.W.C. 2010. Arctic amplification: can the past predict the future? *Quaternary Science Reviews* 29: 1679–1715.
- MORAN K., BACKMAN J., BRINKHUIS H., CLEMENS S., CRONIN T., DICKENS G., EYNAUD F., GATTACCECA J., JAKOBSSON M., JORDAN R., KAMINSKI M., KING J., KOC N., KRYLOV A., MARTINEZ N., MATTHIESSEN J., MOORE T., ONODERA J., O'REGAN M., PÄLIKE H., REA B., Rio D., SAKAMOTO T., SMITH D., STEIN R., St. JOHN K., SUTO I., SUZUKI N., TAKAHASHI K., WATANABE M., YAMAMOTO M., FRANK M., KUBIK P., JOKAT W., KRISTOFFERSEN Y., MCINROY D. and FARRELL J. 2006. The Cenozoic palaeoenvironment of the Arctic Ocean. *Nature* 441: 601–605.
- MOSKALIK M. and BIALIK R. 2011. Statistical analysis of topography of Isvika Bay, Murchisonfjorden, Svalbard. In: P. Rowinski (ed.) *30th International School of Hydraulics 14–17.09.2010, Wiejce Palace, Skwierzyna, Poland. GeoPlanet: Earth and Planetary Sciences, Experimental Methods in Hydraulic Research*: 225–233
- MOSKALIK M., PASTUSIAK T. and TEGOWSKI J. 2012. Multibeam bathymetry and slopes stability of Isvika Bay, Murchisonfjorden, Nordaustlandet. *Marine Geodesy* 35: 389–398.
- NILSEN F., COTTIER F., SKOGSETH R. and MATSSON S. 2008. Fjord-shelf exchanges controlled by ice and brine production: The interannual variation of Atlantic Water in Isfjorden, Svalbard. *Continental Shelf Research* 28: 1838–1853.
- OJALA A.E.K., KUBISCHTA F., KAAKINEN A. and SALONEN V.-P. 2011. Characterization of diamictons on the basis of their mineral magnetic properties in Murchisonfjorden, Nordaustlandet, Svalbard. *Sedimentary Geology* 233: 150–158.
- OLDFIELD F. 1991. Environmental magnetism – a personal perspective. *Quaternary Science Reviews* 10: 73–86.
- OTTESEN D. and DOWDESWELL J.A. 2009. An inter-ice-stream glaciated margin: Submarine landforms and a geomorphic model based on marine-geophysical data from Svalbard. *Geological Society of America Bulletin* 121: 1647–1665.

- PAN Y., PETERSEN N., WINKLHOFFER M., DAVILA A.F., LIU Q., FREDERICH S. T., HANZLIK M. and ZHU R. 2005. Rock magnetic properties of uncultured magnetotactic bacteria. *Earth and Planetary Science Letters* 237: 311–325.
- PETERMANN H. and BLEIL U. 1993. Detection of live magnetotactic bacteria in deep-sea sediments South Atlantic. *Earth and Planetary Science Letters* 117: 223–228.
- POHJOLA V.A., KANKAANPÄÄ P., MOORE J.C. and PASTUSIAK T. 2011. The International Polar Year project “KINNVIKA”-Arctic warming and impact research at 80°N. *Geografiska Annaler, Series A, Physical Geography* 93: 201–208.
- POLYAK L., ALLEY R.B., ANDREWS J.T., BRIGHAM-GRETTE J., CRONIN T.M., DARBY D.A., DYKE A.S., FITZPATRICK J.J., FUNDER S., HOLLAND M., JENNINGS A.E., MILLER G.H., O’REGAN M., SAVELLE J., SERREZE M., ST. JOHN K., WHITE J.W.C. and WOLFF E. 2010. History of sea ice in the Arctic. *Quaternary Science Reviews* 29: 1757–1778.
- RASMUSSEN T.L. and THOMASEN E., 2009. Stable isotope signals from brines in the Barents Sea: Implications for brine formation during the last glaciation. *Geology* 37: 903–906.
- REIMER P.J., BAILLIE M.G.L., BARD E., BAYLISS A., BECK J.W., BLACKWELL P.G., BRONK RAMSEY C., BUCK C.E., BURR G., EDWARDS R.L., FRIEDRICH M., GROOTES P.M., GUILDERSON T.P., HAJDAS I., HEATON T.J., HOGG A.G., HUGHEN K.A., KAISER K.F., KROMER B., MCCORMAC F.G., MANNING S.W., REIMER R.W., RICHARDS D.A., SOUTHON J., TURNEY C.S.M., VAN DER PLICHT J. and WEYHENMEYER C. 2009. IntCal09 and Marine09 radiocarbon age calibration curves, 0–50,000 years cal BP. *Radiocarbon* 51: 1111–1150.
- SANDELIN S., TEBENKOV A.M. and GEE D.G. 2001. The stratigraphy of the lower part of the Neoproterozoic Murchisonfjorden Supergroup in Nordaustlandet, Svalbard. *GFF* 123: 113–127.
- SANDGREN P. and SNOWBALL I.F. 2001. Application of mineral magnetic techniques to paleolimnology. In: W.M. Last and J.P. Smol (eds) *Developments in Paleoenvironmental Research. Tracking Environmental Change Using Lake Sediments*, Volume 2: Physical and Geochemical Methods. Kluwer Academic Publisher, Dordrecht: 217–237.
- SKIRBEKK K., KLITGAARD-KRISTENSEN D., RASMUSSEN T.L., KOÇ N. and FORWICK M. 2010. Holocene climate variations at the entrance to a warm Arctic fjord: evidence from Kongsfjorden trough, Svalbard. *Geological Society, London, Special Publications* 344: 289–304.
- SMITH L.M. and ANDREWS J.T. 2000. Sediment characteristics in iceberg dominated fjords, Kangerlussuaq region, East Greenland. *Sedimentary Geology* 130: 11–25.
- SOLOMON S., QIN D., MANNING M., CHEN Z., MARQUIS M., AVERYT K.B., TIGNOR M. and MILLER H.L. (eds) 2007. *Contribution of Working Group I to the Fourth Assessment Report of the Intergovernmental Panel on Climate Change, 2007*. Cambridge University Press, Cambridge: 996 pp.
- STUIVER M. and BRAZIUNAS T.F. 1993. Modeling atmospheric ¹⁴C influences and ¹⁴C ages of marine samples to 10,000 BC. *Radiocarbon* 35: 137–189.
- SVENDSEN H., BESZCZYNSKA-MØLLER A., HAGEN J.O., LEFAUCCONNIER B., TVERBERG V., GERLAND S., ØRBÆK J.B., BISCHOF K., PAPUCCI C., ZAJĄCZKOWSKI M., AZZOLINI R., BRULAND O., WIENCKE C., WINTHER J.-G. and DALLMANN W. 2002. The physical environment of Kongsfjorden-Krossfjorden, an Arctic fjord system in Svalbard. *Polar Research* 21: 133–166.
- SZCZUCIŃSKI W., ZAJĄCZKOWSKI M. and SCHOLTEN J. 2009. Sediment accumulation rates in sub-polar fjords – Impact of post-Little Ice Age glaciers retreat, Billefjorden, Svalbard. *Estuarine, Coastal and Shelf Science* 85: 345–356.
- ŚLUBOWSKA M.A., KOÇ N., RASMUSSEN T.L. and KLITGAARD-KRISTENSEN D. 2005. Changes in the flow of Atlantic water into the Arctic Ocean since the last deglaciation: Evidence from the northern Svalbard continental margin, 80 N. *Paleoceanography* 20: 1–15.
- THOMPSON R. and OLDFIELD F. 1986. *Environmental magnetism*. Allen & Unwin, London: 227 pp.
- THOMPSON R., BLOEMENDAL J., DEARING J.A., OLDFIELD F., RUMMERY T.A., STOBER J.C. and TURNER G.M. 1980. Environmental applications of magnetic measurements. *Science* 207: 481–486.

- WERNER K., SPIELHAGEN R.F., BAUCH D., HASS C., KANDIANO E. and ZAMELCZYK K. 2011. Atlantic Water advection to the eastern Fram Strait – Multiproxy evidence for late Holocene variability. *Palaeogeography, Palaeoclimatology, Palaeoecology* 308: 264–276.
- ZAJĄCZKOWSKI M. 2008. Sediment supply and fluxes in glacial and outwash fjords, Kongsfjorden and Adventfjorden, Svalbard. *Polish Polar Research* 29: 59–72.
- ZAJĄCZKOWSKI M. and WŁODARSKA-KOWALCZUK M. 2007. Dynamic sedimentary environments of an Arctic glacier-fed river estuary (Adventfjorden, Svalbard). I. Flux, deposition, and sediment dynamics. *Estuarine, Coastal and Shelf Science* 74: 285–296.
- ZAJĄCZKOWSKI M., BOJANOWSKI R. and SZCZUCIŃSKI W. 2004. Recent changes in sediment accumulation rates in Adventfjorden, Svalbard. *Oceanologia* 46: 217–231.
- ZAJĄCZKOWSKI M., SZCZUCIŃSKI W., PLESSEN B. and JERNAS P. 2010. Benthic foraminifera in Hornsund (Svalbard): Implication on paleoenvironmental reconstructions. *Polish Polar Research* 31: 349–375.

Received 22 October 2013

Accepted 20 February 2014